The 2010 IEEE/RSJ International Conference on
Intelligent Robots and Systems
October 18-22, 2010, Taipei, Taiwan

# Motion Control of Passive Mobile Robot with Multiple Casters Based on Feasible Braking Force and Moment

Masao Saida, Yasuhisa Hirata and Kazuhiro Kosuge

*Abstract*— **We introduce a passive mobile robot called C-PRP (Caster-type Passive Robot Porter). This robot consists of multiple casters with servo brakes and a controller. C-PRP employs passive dynamics with respect to the force applied by a human. Its appropriate motion is controlled using the servo brakes. In this paper, we derive and analyze a feasible braking force/moment that can be applied to the robot on the basis of the characteristics of the servo brakes. In addition, we propose a motion control algorithm for C-PRP based on the analysis of this feasible braking force/moment. This algorithm is independent of the number of casters. The proposed algorithm is applied to a four-wheeled C-PRP and the experimental results confirm its validity.**

## I. Introduction

Robots are expected to flourish in the medical/welfare field, and the human living environment to work in cooperation with humans. Many researchers have studied human-robot cooperation issues [1]-[5]. The safety of users utilizing robot systems in these environments must be taken into consideration. Most robots use servo motors to control their motion. As such, if these servo motors cannot be appropriately controlled, the robots may perform undesired movements and could potentially pose a safety threat.

From a safety point of view, Goswami et al. proposed the concept of passive robotics in which a system moves passively based on external force/moment without using servo motors [6]. Peshkin et al. developed an object handling system called Cobot [7] that consists of non-offset casters and controls only the steering angles with the servo motors. Wasson et al. [8] and Rentschler et al. [9] also proposed passive intelligent walkers.

We too developed a passive intelligent walker called RT Walker to support the walking of people with disabilities and the elderly [10]. It differs from other passive robots in that it controls the servo brakes attached to wheels appropriately to realize several functions without the use of servo motors. We also developed a passive object handling robot called O-PRP (Omnidirectional-wheel-type Passive Robot Porter) [11]-[13]. O-PRP consists of three omnidirectional wheels with servo brakes. It also controls its own motion using the servo brakes as RT Walker does. These passive systems are intrinsically safe because they cannot move unintentionally with driving force. It is expected that passive robotics will continue to prove useful in many types of intelligent systems that employ physical interaction between systems and humans.

In this research, we extended the brake control technologies of the RT Walker and the O-PRP to the control of a new passive mobile robot. This robot is called C-PRP (Caster-type Passive Robot Porter). A caster has two rotary shafts: a wheel shaft and a pivot shaft. The pivot shaft is placed away from the wheel shaft at the length of the offset. A caster can move in all directions, like an omnidirectional wheel, because the pivot shaft rotates passively on the basis of external force/moment. However, a caster has certain advantages over an omnidirectional wheel: it moves with less vibration, has a high withstand load, and offers high step-climbing performance. Given this, casters are widely used for moving many kinds of objects in our daily lives.

The control of casters based on the concept of passive robotics will enable us to develop several kinds of passive-type moving bases depending on the applications. We could also add numerous functions such as collision avoidance and path tracking to the moving bases with casters that are widely used in the real world. For example, we could realize safety and high performance in an object handling system that deals with large, long, or complicated shaped objects.

In previous studies, we developed a prototype C-PRP consisting of two casters with servo brakes and one passive rigid wheel. We also proposed a fundamental motion control algorithm for this robot system [14]. In this system, the rigid wheel constrained the motion in the axial direction according to the nonholonomic constraint. Therefore, we could achieve motion control of this system by controlling the two casters with servo brakes. However, this algorithm was adjusted only to this system.

Fig. 1. Caster Type Passive Robot Porter (C-PRP)

M. Saida, Y. Hirata and K. Kosuge are with Derartment of Bioengineering and Robotics, Tohoku University, 6-6-01, Aoba, Aramaki, Aoba-ku, Sendai 980-8579, JAPAN {saida, hirata, kosuge}@irs.mech.tohoku.ac.jp

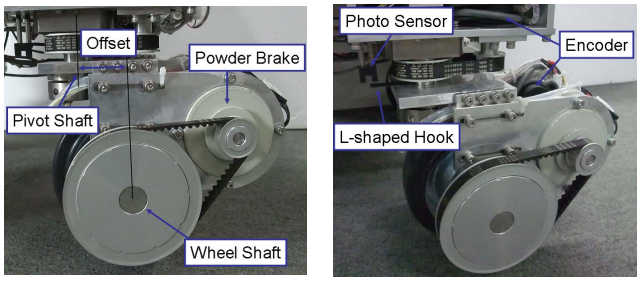


Fig. 2. Caster with Servo Brake

In contrast, when we transport an object using a moving base consisting of casters, we can arbitrarily choose the number of casters on the basis of the weight or shape of an object. It is thus advisable that the motion control algorithm of C-PRP be independent of the number of casters.

In the next section, we first introduce the new C-PRP that consists of multiple casters with servo brakes; it can move in all directions. Next, we discuss the characteristics of C-PRP. Specifically, we derive and analyze the feasible braking force/moment applied to the robot on the basis of the characteristics of the servo brakes. In addition, we propose a motion control algorithm that is adaptable to C-PRP, consisting of multiple casters, based on the analysis of the feasible braking force/moment. Finally, the proposed algorithm is applied to a four-wheeled C-PRP, and the experimental results confirm the validity of the proposed algorithm.

## II. Caster Type Passive Robot Porter (C-PRP)

We developed a passive mobile robot with casters called C-PRP based on the concept of passive robotics [6], shown in Fig. 1. The caster with a servo brake is shown in Fig. 2. A servo brake is installed only in the wheel shaft of each caster because free rotation of the pivot shaft is important in this passive system.

Two encoders are also installed on the wheel shaft and the pivot shaft of each caster for odometry. These encoders are incremental encoders that allow measurement of the relative position of the shaft. However, this system needs to measure the absolute position of each pivot shaft, thus a U-shaped micro photo sensor and an L-shaped hook are attached to each caster, as shown in Fig. 2. We can initialize the encoder information by using them and we can determine the absolute position of each pivot shaft.

The control performance of the robot depends on the characteristics of the servo brakes. We used Powder Brake (Mitsubishi Corp., ZKG-20YN, maximum on-state torque: 2.0[Nm]) as the servo brake. It provides high reliability in terms of responsiveness and good linearity in controlling the wheel braking torque.

## III. Characteristics of C-PRP

### A. Control Condition of Servo Brake

C-PRP moves solely on the basis of the external force and moment applied to it as it does not have any servo motors.

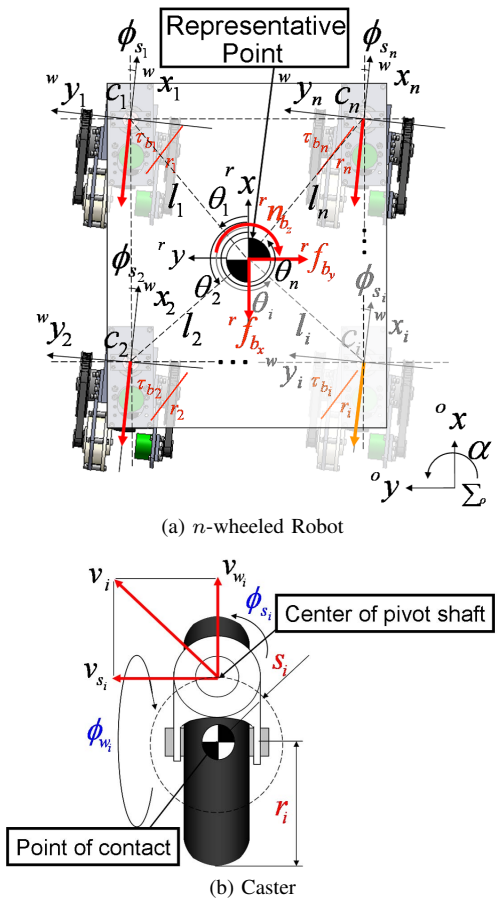


(a) $n$-wheeled Robot

(b) Caster

Fig. 3. Coordinate System of C-PRP

This is a very important safety feature. The characteristics of a brake-wheel system are significantly more complicated compared to a motor-wheel system. The characteristics of the brake system depend on wheel rotational direction. The direction of wheel rotation determines the sign of the wheel's output torque. The magnitude of the torque is proportional to the input current of the brake. The following condition exists between the angular velocity of the wheel and the braking torque of the servo brake.

$$\tau_{b_i}\dot{\phi}_{w_i} \leq 0 \quad (i \in 1, \cdots, n) \tag{1}$$

where $\tau_{b_i}$ is the braking torque generated by the servo brake, $\dot{\phi}_{w_i}$ is the angular velocity of the wheel, and $n$ is the number of casters. This condition is the servo brake control constraint; it indicates that a servo brake cannot generate arbitrary torque. Therefore, we need to consider the direction of wheel rotation and the feasible braking torque $\tau_{b_i}$ during motion control of a robot.

### B. Feasible Braking Force and Moment

The servo brake control constraint, as mentioned in the section $A$, influences the feasible braking force/moment applied to the robot. First, the set $V$ of the torque $\boldsymbol{\tau}_m$ with

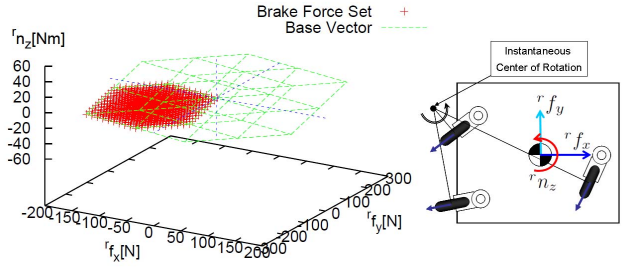


(a) ${}^r f_x$—${}^r f_y$—${}^r n_z$

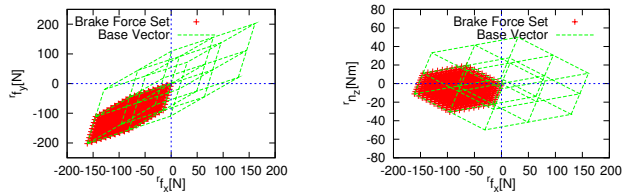


(b) ${}^r f_x$—${}^r f_y$ (c) ${}^r f_x$—${}^r n_z$

$(\phi_{s_1} = 80°, \phi_{s_2} = 45°, \phi_{s_3} = 30°)$

Fig. 4. Feasible Braking Force and Moment Set $B(U)$ (Ex.1)

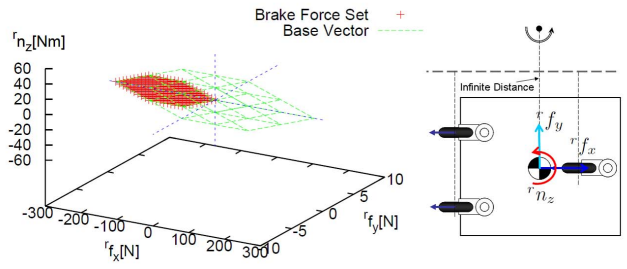


(a) ${}^r f_x$—${}^r f_y$—${}^r n_z$

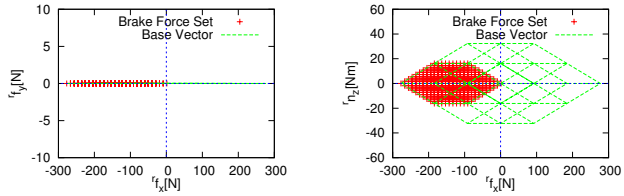


(b) ${}^r f_x$—${}^r f_y$ (c) ${}^r f_x$—${}^r n_z$

$(\phi_{s_1} = 0°, \phi_{s_2} = 0°, \phi_{s_3} = 0°)$

Fig. 5. Feasible Braking Force and Moment Set $B(U)$ (Ex.2)

servo motors is shown as follows:

$$V = \{ \sum_{i=1}^{n} \tau_{m_i} \boldsymbol{e}_i \mid |\tau_{m_i}| \leq \tau_{max} \quad (i \in 1, \cdots, n) \} \tag{2}$$

where

$$\begin{bmatrix} \boldsymbol{e}_1 & \cdots & \boldsymbol{e}_n \end{bmatrix} = diag(1, \cdots, 1) \tag{3}$$

However, all torques in this set $V$ are not feasible using the servo brakes. The feasible braking torque set $U$ is derived by considering the servo brake control constraint in Eq. (1) as follows:

$$U = \{ \sum_{i=1}^{n} \tau_{b_i} \boldsymbol{e}_i \mid |\tau_{b_i}| < \tau_{max}, \ \tau_{b_i} \dot{\phi}_{w_i} \leq 0 \quad (i \in 1, \cdots, n) \} \tag{4}$$

In conventional research on O-PRP, we have classified the motion of the robot on the basis of the signs of the wheels' angular velocities. In each motion type, the servo brake control constraint in Eq. (1) should be considered in the derivation of the feasible braking torques. In this system, however, the casters change their direction passively on the basis of external force/moment. Therefore, the wheels of all casters rotate in a constant direction except for singular motion such as the turning movement of casters. For simplicity, in this paper, we assume that the rotational direction of each caster's wheel is constant. We only consider the case of this motion type.

Next, we consider the relation between the braking torques and the braking force/moment. The robot coordinate system of $n$-wheeled C-PRP is set at the center of the polygon configured by the points $c_i$ of pivot shafts, as shown in Fig. 3(a). We define the resultant braking force/moment applied to the robot with respect to the $\sum_r$ as ${}^r \boldsymbol{F}_b = \begin{bmatrix} {}^r f_{b_x} & {}^r f_{b_y} & {}^r n_{b_z} \end{bmatrix}^T$. We can express the relation between the braking torque $\boldsymbol{\tau}_b = \begin{bmatrix} \tau_{b_1} & \cdots & \tau_{b_n} \end{bmatrix}^T$ and the resultant braking force/moment ${}^r \boldsymbol{F}_b$ applied to the robot as follows:

$${}^r \boldsymbol{F}_b = \boldsymbol{A} \boldsymbol{\tau}_b \tag{5}$$

where

$$\boldsymbol{A} = \begin{bmatrix} A_1 & \cdots & A_n \end{bmatrix} \tag{6}$$

$$A_i = {}^1/_{r_i} \begin{bmatrix} \cos\phi_{s_i} & \sin\phi_{s_i} & l_i \sin(\phi_{s_i} - \theta_i) \end{bmatrix}^T \tag{7}$$

where $r_i$ denotes the radius of each wheel, and $\phi_{s_i}$ denotes the angle of each pivot shaft, as shown in Fig. 3(b). $l_i$ denotes the distance between the origin ${}^r o$ and each pivot shaft. $\theta_i$ denotes the angle between ${}^r x$-axis and $\overrightarrow{{}^r o c_i}$.

We can derive the feasible braking force/moment set $B(U)$ from the feasible braking torque set $U$ and Eq. (5) as follows:

$$B(U) = \{ \sum_{i=1}^{n} \tau_{b_i} \boldsymbol{v}_i \mid \tau_{b_i} \in U \ (i \in 1, \cdots, n) \} \tag{8}$$

where

$$\begin{bmatrix} \boldsymbol{v}_1 & \cdots & \boldsymbol{v}_n \end{bmatrix}^T = \boldsymbol{A} \begin{bmatrix} \boldsymbol{e}_1 & \cdots & \boldsymbol{e}_n \end{bmatrix}^T \tag{9}$$

Figure 4 shows the sets of $B(U)$ and $B(V)$ when each caster's angle of three-wheeled C-PRP is $\phi_{s_1} = 80°$, $\phi_{s_2} = 45°$, and $\phi_{s_3} = 30°$, respectively. $B(U)$ is a subset of $B(V)$. Note that the three axes of the coordinate in Fig. 4(a) express the forces ${}^r f_x$, ${}^r f_y$ and moment ${}^r n_z$ on the robot coordinate system. The two axes in Fig. 4(b) express ${}^r f_x$ and ${}^r f_y$. The two axes in Fig. 4(c) express ${}^r f_x$ and ${}^r n_z$.

### C. Analysis of Feasible Braking Force and Moment

Here, we focus on Eq. (5), which derives the braking force/moment ${}^r \boldsymbol{F}_b$ from the feasible braking torque $\boldsymbol{\tau}_b$. The feasible braking force/moment set $B(U)$ changes on the basis of the direction of casters $\phi_{s_i}$ in real time because matrix

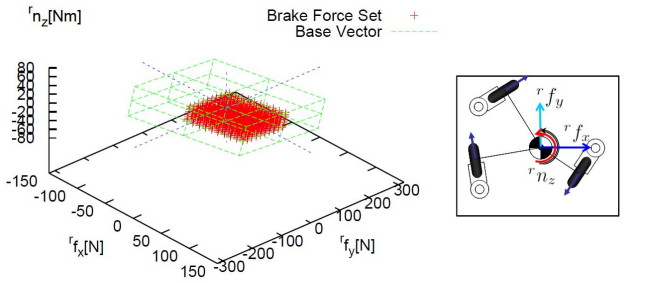


(a) ${}^{r}f_x$—${}^{r}f_y$—${}^{r}n_z$

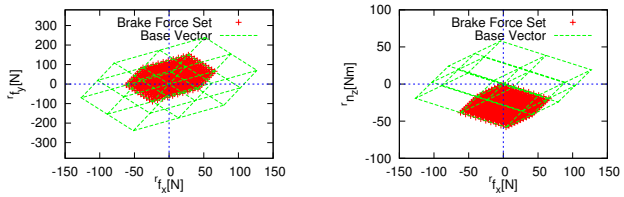


(b) ${}^{r}f_x$—${}^{r}f_y$ (c) ${}^{r}f_x$—${}^{r}n_z$

$(\phi_{s_1} = 75°, \phi_{s_2} = 225°, \phi_{s_3} = 294°)$

Fig. 6. Feasible Braking Force and Moment Set $B(U)$ (Ex.3)

$\boldsymbol{A}$ is a function of $\phi_{s_i}$ in Eq. (5). Therefore, in this section, we analyze the change of the feasible braking force/moment set $B(U)$ in more detail. In addition to the aforementioned example shown in Fig. 4, two more examples of the feasible braking force/moment sets $B(U)$ are shown in Figs. 5 and 6. Figures 4 and 5 show examples of object transportation to another place. Figure 6 shows an example of C-PRP orientation change.

In this paper, we assume that the motion of C-PRP has an instantaneous center of rotation $x_{ICR}$ during movement, as shown in Fig. 4(a). Example 1 is a case in which $x_{ICR}$ is near the robot, as shown in Fig. 4. Example 2 is a case in which $x_{ICR}$ is at infinity, as shown in Fig. 5. Example 3 is a case in which $x_{ICR}$ is the origin ${}^{r}o$ of the robot coordinate system, as shown in Fig. 6.

First, we focus on the feasible braking forces on the ${}^{r}f_x{}^{r}f_y$ plane. Figures 4(b) and 5(b) show that the direction of the feasible braking force is limited. Furthermore, Fig. 5(b) shows that the system can generate braking force only in one direction during rectilinear travel because C-PRP performs a singular motion and all casters of C-PRP face in the same direction. In contrast, Fig. 6(b) shows that the feasible braking force is generated omnidirectionally.

Next, we consider the moment ${}^{r}n_z$. Figures 4(c) and 5(c) show that the moment is generated in both directions. Figure 6(c), however, shows that the moment is generated only in the opposite direction of the robot's rotational direction.

It is thus evident that, in order to generate the feasible braking force/moment properly, we need to consider the current motion of the system, which includes the following two factors: the sign of the angular velocities of wheels and the direction of casters.

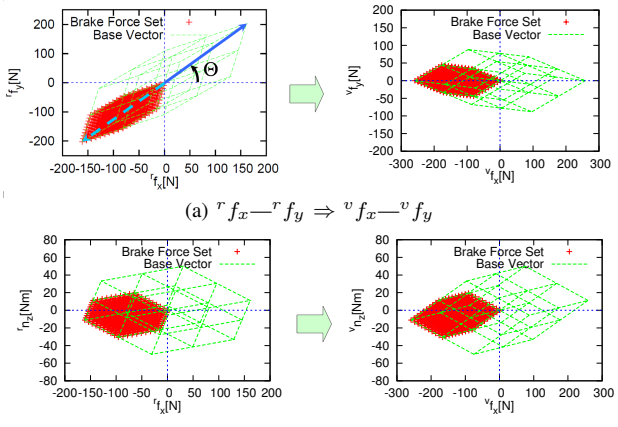


(a) ${}^{r}f_x$—${}^{r}f_y$ $\Rightarrow$ ${}^{v}f_x$—${}^{v}f_y$

(b) ${}^{r}f_x$—${}^{r}n_z$ $\Rightarrow$ ${}^{v}f_x$—${}^{v}n_z$

$(\phi_{s_1} = 80°, \phi_{s_2} = 45°, \phi_{s_3} = 30°)$

Fig. 7. Coordinate Transform of Feasible Braking Force and Moment Set $B(U)$ (Ex.1)

## IV. Motion Control of C-PRP based on Feasible Braking Force and Moment

### A. "Reference Direction" for Control of C-PRP

As mentioned in section III C, the feasible braking force/moment changes on the basis of the direction of casters in real time. Here, we consider the case of object transportation to another place. As shown in Figs. 4(b) and 5(b), on the ${}^{r}f_x{}^{r}f_y$ plane, the feasible braking force can be generated sufficiently in a certain direction. However, it is limited to the direction perpendicular to this direction.

Given this, we define the reference direction for control of C-PRP based on the feasible braking force/moment. We define the reference direction for control of C-PRP as the opposite direction of the direction in which the biggest braking force can be generated on the ${}^{r}f_x{}^{r}f_y$ plane, as shown in Fig. 7(a). In fact, this reference direction is approximately the same as that of the robot's velocity in the case of object transportation to another place. For simplicity, we transform the coordinate axes on the basis of the reference direction as follows:

$$\begin{bmatrix} {}^{v}f_x \\ {}^{v}f_y \\ {}^{v}n_z \end{bmatrix} = \begin{bmatrix} \cos\Theta & \sin\Theta & 0 \\ -\sin\Theta & \cos\Theta & 0 \\ 0 & 0 & 1 \end{bmatrix} \begin{bmatrix} {}^{r}f_x \\ {}^{r}f_y \\ {}^{r}n_z \end{bmatrix} \tag{10}$$

where ${}^{v}f_x$, ${}^{v}f_y$ and ${}^{v}n_z$ denote the force and moment with respect to the coordinate system $\sum_v$ based on the reference direction, respectively. Figure 7 shows the coordinate transform of the feasible braking force/moment set $B(U)$ of Ex. 1 shown in Fig. 4.

### B. Concept of Motion Control for Passive Mobile Robot with Servo Brakes

Next, we consider controlling C-PRP by using the force ${}^{v}f_x$ and the moment ${}^{v}n_z$. In this section, we explain how to generate the braking force/moment based on the feasible braking force/moment set [11]. We define ${}^{v}\boldsymbol{F}_d$ and

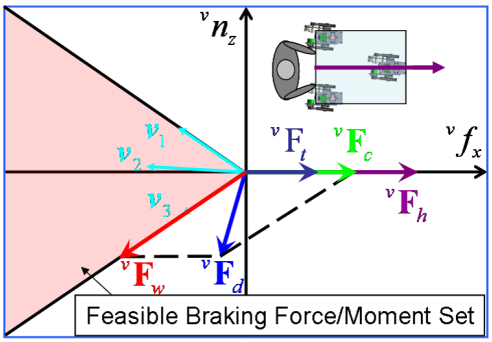


Fig. 8. Control of Robot Based on Feasible Braking Force and Moment

${}^v\boldsymbol{F}_w$ as the desired force/moment and the feasible braking force/moment, respectively. The desired force/moment ${}^v\boldsymbol{F}_d$ should be generated and determined in real time by a control law such as motion control for path tracking, obstacle collision avoidance, and impedance control.

If the desired force/moment ${}^v\boldsymbol{F}_d$ is within the feasible braking force/moment set $B(U)$, we can command the braking torques of the wheels directly as ${}^v\boldsymbol{F}_w = {}^v\boldsymbol{F}_d$.

Next, we consider the case that ${}^v\boldsymbol{F}_d$ is out of the feasible braking force/moment set $B(U)$. In this research, a human operator applies a force to the robot by pushing it. The force/moment ${}^v\boldsymbol{F}_h$ applied by the human can be divided into two elements. One is the driving force ${}^v\boldsymbol{F}_t$ utilized for moving the robot in the reference direction, and the other is the compensating force/moment ${}^v\boldsymbol{F}_c$. The following equation illustrates this relation.

$$ {}^v\boldsymbol{F}_h = {}^v\boldsymbol{F}_t + {}^v\boldsymbol{F}_c \tag{11} $$

The compensating force/moment ${}^v\boldsymbol{F}_c$ generates a force/moment that the feasible braking force/moment ${}^v\boldsymbol{F}_w$ cannot for generating the desired force/moment ${}^v\boldsymbol{F}_d$. In other words, we can achieve the desired force/moment ${}^v\boldsymbol{F}_d$ by composition of the feasible braking force/moment ${}^v\boldsymbol{F}_w$ and the compensating force/moment ${}^v\boldsymbol{F}_c$, as shown in Fig. 8. Equation (12) illustrates this relation.

$$ {}^v\boldsymbol{F}_d = {}^v\boldsymbol{F}_w + {}^v\boldsymbol{F}_c \tag{12} $$

As a result, we can express the dynamics of C-PRP as follows:

$$ \boldsymbol{M}\ {}^v\ddot{\boldsymbol{q}} + \boldsymbol{D}\ {}^v\dot{\boldsymbol{q}} = {}^v\boldsymbol{F}_t + {}^v\boldsymbol{F}_d \tag{13} $$

where

$$ \boldsymbol{M} = \begin{bmatrix} m & 0 \\ 0 & J \end{bmatrix}, \boldsymbol{D} = \begin{bmatrix} D & 0 \\ 0 & D_\theta \end{bmatrix}, {}^v\boldsymbol{q} = \begin{bmatrix} {}^vx \\ \alpha \end{bmatrix} \tag{14} $$

where $\boldsymbol{M} \in \boldsymbol{R}^{2\times 2}$ is the inertia matrix, $\boldsymbol{D} \in \boldsymbol{R}^{2\times 2}$ is the damping matrix, and ${}^v\boldsymbol{q}$ is a position and an orientation of C-PRP with respect to the $\sum_v$. This equation means that C-PRP is moved on the basis of the driving force ${}^v\boldsymbol{F}_t$ for moving the robot in the reference direction and the desired force/moment ${}^v\boldsymbol{F}_d$ for realizing several functions.

Thus, we need to derive the feasible braking force/moment ${}^v\boldsymbol{F}_w$ within the braking force/moment set $B(U)$ on the basis of the relation expressed by Eq. (12).

### C. Motion Control Algorithm for C-PRP

A caster can move in all directions because the pivot shaft rotates passively on the basis of external force/moment. When we transport an object using a moving base consisting of casters, we can choose the number of casters flexibly on the basis of the weight or shape of an object. Therefore, it is advisable for the motion control algorithm of C-PRP to be independent of the number of casters.

This algorithm is based on the concept of motion control for the passive mobile robot, as mentioned in the previous section. We also consider deriving the feasible braking force/moment ${}^v\boldsymbol{F}_w$ as the compensating force/moment ${}^v\boldsymbol{F}_c$ becomes as small as possible.

Figure 9 presents a flow chart of the motion control algorithm for C-PRP. First, the desired force/moment ${}^v\boldsymbol{F}_d = \begin{bmatrix} {}^vf_{d_x} & {}^vn_{d_z} \end{bmatrix}^T$ is determined by the control law applied to the system. Next, we redefine matrix $\boldsymbol{A}$ in order to control C-PRP by using the force ${}^vf_x$ and the moment ${}^vn_z$ as follows:

$$ \boldsymbol{A} = \begin{bmatrix} \cos(\phi_{s_1} - \Theta) & \cdots & \cos(\phi_{s_n} - \Theta) \\ l_1 \sin(\phi_{s_1} - \theta_1) & \cdots & l_n \sin(\phi_{s_n} - \theta_n) \end{bmatrix} \in \boldsymbol{R}^{2\times n} \tag{15} $$

We derive the braking torque $\boldsymbol{\tau}_b$ using new $\boldsymbol{A}$ as follows:

$$ \boldsymbol{\tau}_b = \boldsymbol{A}^\dagger {}^v\boldsymbol{F}_d + (\boldsymbol{I} - \boldsymbol{A}^\dagger \boldsymbol{A})\boldsymbol{k} \tag{16} $$

where $\boldsymbol{A}^\dagger \in \boldsymbol{R}^{n\times 2}$ is the pseudoinverse matrix of $\boldsymbol{A}$, $\boldsymbol{k} \in \boldsymbol{R}^n$ is an arbitrary constant vector, and $\boldsymbol{I} \in \boldsymbol{R}^{n\times n}$ is a unit vector. In fact, in this paper, we define $\boldsymbol{k} = \boldsymbol{0}$. In future work, we will consider the control using the redundancy of the robot by choosing $\boldsymbol{k}$ on the basis of a control law. Using the pseudoinverse matrix of $\boldsymbol{A}$, we can derive the braking torque $\boldsymbol{\tau}_b$ independently of the number of casters.

Further, we determine whether or not the braking torque $\boldsymbol{\tau}_b$ derived from Eq. (16) meets the servo brake control constraint shown in Eq. (1). If all of the braking torques $\boldsymbol{\tau}_b$ meet this condition, then ${}^v\boldsymbol{F}_d$ is within the feasible braking force/moment set $B(U)$. Therefore, we can command the braking torques of the wheels directly.

However, if even a single braking torque of $\boldsymbol{\tau}_b$ does not satisfy this condition, we consider realizing ${}^v\boldsymbol{F}_d$ by composition of the feasible braking force/moment ${}^v\boldsymbol{F}_w$ and the compensating force/moment ${}^v\boldsymbol{F}_c$. First, we redefine $\boldsymbol{A}$ as $\boldsymbol{A}'$ and $\boldsymbol{\tau}_b$ as $\boldsymbol{\tau}_{b+h}$ as follows:

$$ \boldsymbol{A}' = \begin{bmatrix} \boldsymbol{A} & \lambda_{h_x} & 0 \\ & 0 & \lambda_{h_z} \end{bmatrix} \in \boldsymbol{R}^{2\times(n+2)} \tag{17} $$

$$ \boldsymbol{\tau}_{b+h} = [\tau_{b_1} \quad \cdots \quad \tau_{b_n} \quad {}^vf_{h_x} \quad {}^vn_{h_z}]^T \in \boldsymbol{R}^{(n+2)} \tag{18} $$

where $\lambda_{h_x}$ and $\lambda_{h_z}$ are constant: 0 or 1, respectively. They decide whether we can utilize the compensating force ${}^vf_{c_x}$ or the compensating moment ${}^vn_{c_z}$ or not. In this paper, we define $\lambda_{h_x} = 1$ and $\lambda_{h_z} = 0$ because we assume that the human operator applies the compensating force

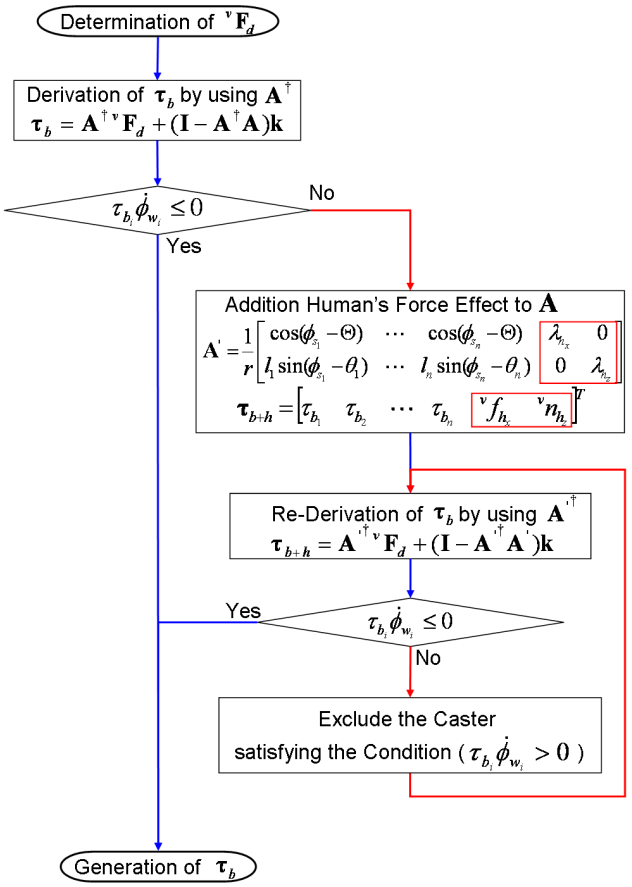


Fig. 9. Flow Chart of Motion Control Algorithm for C-PRP

only in the reference direction and does not apply the compensating moment. In fact, if the system can determine the force/moment applied by the human using the force sensor, the compensating moment ${}^{v}n_{a_z}$ can also be used for control by defining $\lambda_{h_z} = 1$. We recalculate the braking torque $\boldsymbol{\tau}_{b+h}$ using Eqs. (16), (17), and (18).

Nevertheless, when even a single braking torque of $\boldsymbol{\tau}_b$ does not satisfy the condition, we exclude the caster not satisfying the condition for control. Specifically, we define the switch matrix $\boldsymbol{A}_s$ and redefine $\boldsymbol{A}'$ as $\boldsymbol{A}''$ as follows:

$$\boldsymbol{A}'' = \boldsymbol{A}'\boldsymbol{A}_s \tag{19}$$

where

$$\boldsymbol{A}_s = \begin{bmatrix} s_{A_1} & & \mathbf{0} & \\ & \ddots & & \mathbf{0} \\ \mathbf{0} & & s_{A_n} & \\ & \mathbf{0} & & \boldsymbol{I}_s \end{bmatrix} \tag{20}$$

where $\boldsymbol{I}_s \in \boldsymbol{R}^{2\times 2}$ is a unit vector and $s_{A_i}(i \in 1, \cdots, n)$ is constant: 0 or 1. If the braking torque $\tau_{b_i}$ does not satisfy the condition ($\tau_{bi}\omega_{wi} \le 0$), we define $s_{A_i} = 0$. If it does, we define $s_{A_i} = 1$. As a result, we can exclude the caster not satisfying the condition for control. This algorithm enables the compensating force/moment to cover the force/moment that should be generated by the braking torque which does not satisfy the condition. Furthermore, the torque $\boldsymbol{\tau}_{b+h}$ derived by the first term of the right-hand side of Eq. (16) was the solution minimizing the Euclidean norm $\|\boldsymbol{\tau}_{b+h}\|$ when the solution is nonunique. As a result, we can derive the feasible braking force/moment ${}^{v}\boldsymbol{F}_w$ to minimize the compensating force/moment ${}^{v}\boldsymbol{F}_c$.

In conclusion, we can realize the desired force/moment ${}^{v}\boldsymbol{F}_d$ through composition of the feasible braking force/moment ${}^{v}\boldsymbol{F}_w$ and the compensating force/moment ${}^{v}\boldsymbol{F}_c$.

## V. Experiment

We applied the algorithm proposed in the previous section to four-wheeled C-PRP, and conducted an experiment to confirm the validity of C-PRP and its control algorithm. In this experiment, we assume that a human operator applies force/moment to C-PRP by pushing it.

### A. Attitude Control

We experimented with four-wheeled C-PRP to achieve a simple attitude control function. In this experiment, we derive the desired moment ${}^{v}n_{d_z}$ to keep the orientation of C-PRP constant as follows:

$${}^{v}n_{d_z} = K_{p\theta}(\alpha_{des} - \alpha) + K_{d\theta}(\dot{\alpha}_{des} - \dot{\alpha}) \tag{21}$$

where $\alpha_{des}$ and $\dot{\alpha}_{des}$ denote the desired orientation and the desired angular velocity of C-PRP, $\alpha$ and $\dot{\alpha}$ are the current orientation and the current angular velocity of C-PRP, and $K_{p\theta}$ and $K_{d\theta}$ are proportional and derivative gains, respectively. We define the desired orientation and the desired angular velocity as $\alpha_{des} = 0$ and $\dot{\alpha_{des}} = 0$, respectively. Thus, the desired force/moment is derived as ${}^{v}\boldsymbol{F}_d = \begin{bmatrix} 0 & {}^{v}n_{d_z} \end{bmatrix}^T$.

In this experiment, a human applies the force/moment to C-PRP through the following five processes:

Step 1: Apply the Moment Intentionally to C-PRP
Step 2: Apply the Force in the ${}^{r}x$ Positive Direction
Step 3: Apply the Force in the ${}^{r}y$ Positive Direction
Step 4: Apply the Force in the ${}^{r}x$ Negative Direction
Step 5: Apply the Moment Intentionally

In addition, we measure the force applied by the human for evaluation of experimental results using the force sensor attached to C-PRP.

The experimental results are illustrated in Figs. 10 to 12. Figure 10(a) shows the path of the robot on the $xy$ plane, Figure 10(b) shows ${}^{v}\boldsymbol{F}_h$ applied by the human. Figures 11(a) and (b) express the orientation of C-PRP and the braking moment applied to C-PRP with respect to time, respectively. Figure 12 shows the motion of the experiment. Figures 13 and 14 express one example of the relation between ${}^{v}\boldsymbol{F}_w$, ${}^{v}\boldsymbol{F}_d$, and ${}^{v}\boldsymbol{F}_h$.

From Figs. 10 and 11, it is evident that C-PRP keeps its own initial orientation although the human applies several types of force/moment to the robot. Figures 13 and 14 show that C-PRP generates the appropriate feasible braking

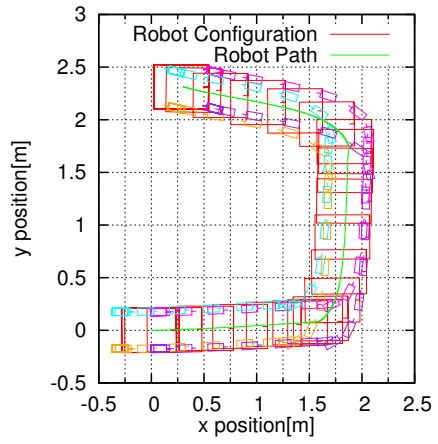


(a) Path of C-PRP

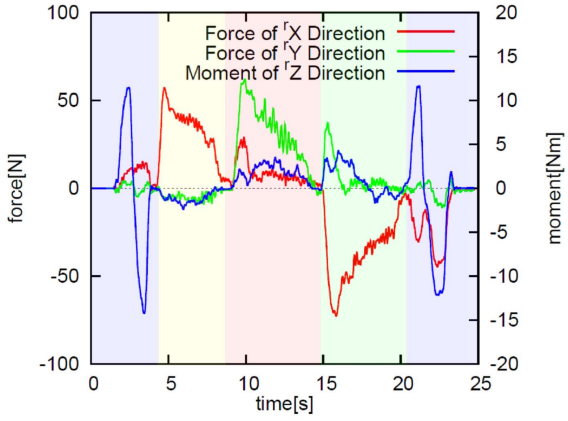


(b) Force Applied by Human

Fig. 10. Experimental Results 1 for Attitude Control

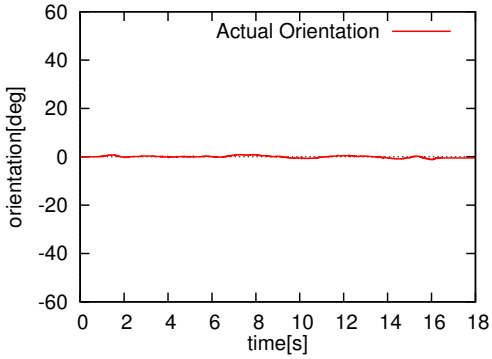


(a) Orientation of C-PRP

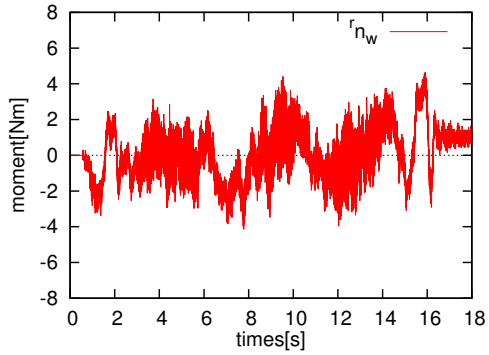


(b) Control Input ${}^{v}n_{w_z}$

Fig. 11. Experimental Results 2 for Attitude Control

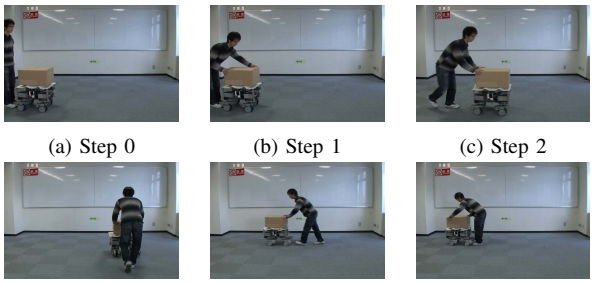

(a) Step 0 (b) Step 1 (c) Step 2

(d) Step 3 (e) Step 4 (f) Step 5

Fig. 12. Experiment for Attitude Control

force/moment. In other words, ${}^{v}\boldsymbol{F}_d$ is realized by composition of ${}^{v}\boldsymbol{F}_w$ and ${}^{v}\boldsymbol{F}_c$. In addition, ${}^{v}\boldsymbol{F}_c$ becomes as small as possible because ${}^{v}\boldsymbol{F}_w$ is generated on the border of Set $B(U)$. C-PRP thus appropriately achieves the desired motion based on the proposed algorithm.

In this experiment, ${}^{v}\boldsymbol{F}_d$ is one example of the force/moment that is obviously located out of the feasible braking force/moment set $B(U)$. Nonetheless, we can achieve ${}^{v}\boldsymbol{F}_d$ by composition of ${}^{v}\boldsymbol{F}_w$ and ${}^{v}\boldsymbol{F}_c$. Therefore, by appropriately determining the desired force/moment by some control law, we can realize several kinds of motion control such as path tracking control, impedance-based motion control, collision avoidance control, and gravity compensation control on a slope, as mentioned in conventional research [10]-[14].

## VI. Conclusion

In this paper, we introduced a caster-type passive object handling robot called C-PRP consisting of multiple casters with servo brakes. We derived the feasible braking force/moment applied to the robot on the basis of the characteristics of the servo brakes. In addition, we analyzed the feasible braking force/moment. On the basis of this analysis, we proposed a motion control algorithm for C-PRP that is independent of the number of casters. The proposed algorithm was applied to four-wheeled C-PRP, and experimental results on the attitude control confirmed its validity.

In the future, we will consider the singularity and redundancy of the robot with many casters to improve the maneuverability of C-PRP. In addition, we will consider modularizing a caster with a servo brake in order to be able to arbitrarily choose the number of casters. Moreover, we currently use servo brakes that can generate sufficient torques for the control of the robot and do not consider maximum torques. By increasing the number of casters, we can use smaller servo brakes and can then consider how to distribute

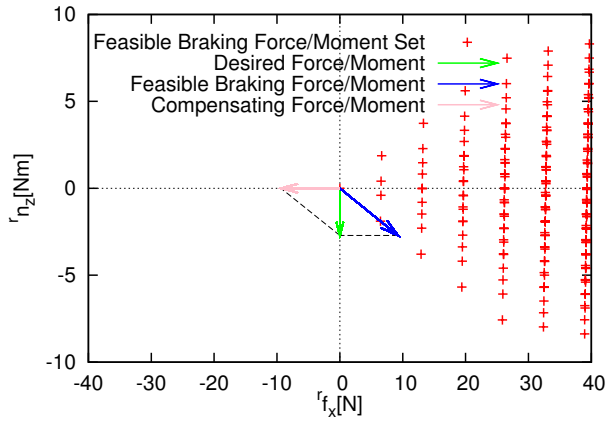


(a) ${}^{r}f_x$ and ${}^{r}n_z$ with respect to the $\sum_r$

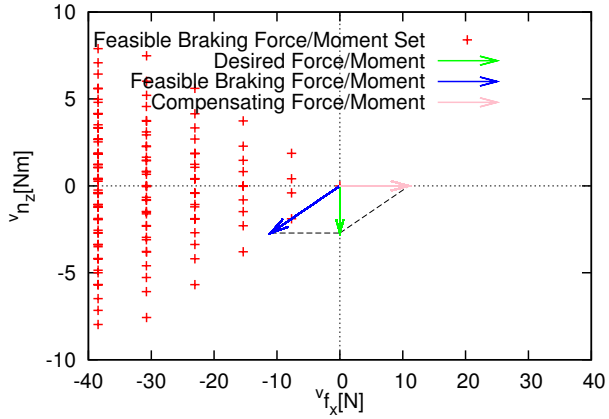


(b) ${}^{v}f_x$ and ${}^{v}n_z$ with respect to the $\sum_v$

Fig. 13. Example of Relation between Feasible Braking, Desired, and Compensating Force/Moment on $f_x n_z$-plane with respect to the $\sum_r$ and $\sum_v$

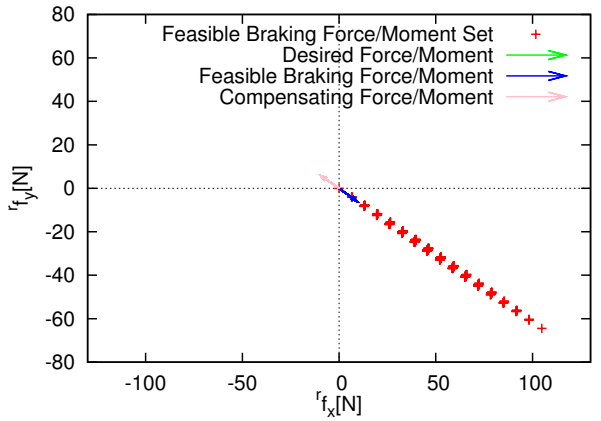


(a) ${}^{r}f_x$ and ${}^{r}f_y$ with respect to the $\sum_r$

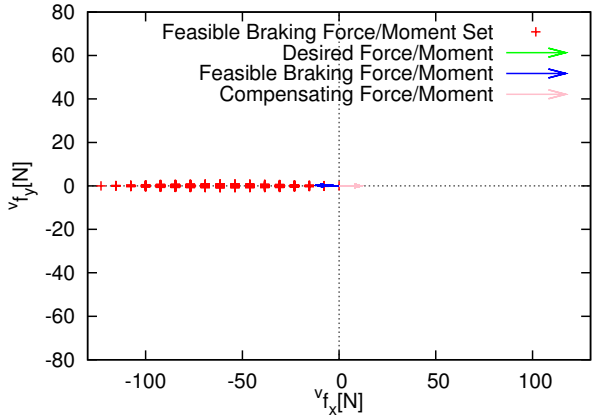


(b) ${}^{v}f_x$ and ${}^{v}f_y$ with respect to the $\sum_v$

Fig. 14. Example of Relation between Feasible Braking, Desired, and Compensating Force/Moment on $f_x f_y$-plane with respect to the $\sum_r$ and $\sum_v$

the braking torque to each caster.

## REFERENCES


[1] O. Khatib, "Mobile manipulation: the robotic assistant", Robotics Autonomous Syst. 26, pp.175-183, 1999.

[2] H. Yabushita, Y. Hirata, K. Kosuge, Z. Wang, "Environment-adaptive control algorithm of power assisted cycle", in: Proc. 29th Annu. Conf. of the IEEE Industrial Electronics Society, Roanoke, VA, Vol. 2, pp.1962-1967, 2003.

[3] Y. Yamada, T. Morizono, Y. Umetani, H. Konosu, "Warning: to err is human working toward a dependable skill-assist with a method for preventing accidents caused by human error", IEEE Robotics Automation Magazine. 11, pp.34-45, 2004.

[4] A. Zoss, H. Kazerooni, "Design of electrically actuated lower extremity exoskeleton", Advanced Robotics 20, pp.967-988, 2006.

[5] T. Takeda, Y. Hirata, K. Kosuge, "Dance step estimation method based on HMM for dance partner robot", IEEE Trans. Ind. Electron. 54, pp.699-706, 2007.

[6] A. Goswami, M. A. Peshkin, J. Colgate, "Passive robotics: an exploration of mechanical computation", Proc. of the IEEE International Conference on Robotics and Automation, pp.279-284, 1990.

[7] M. A. Peshkin, J. E. Colgate, W. Wannasuphoprasit, C. A. Moore, R. B. Gillespie, P.Akella, "Cobot Architecture", IEEE Transactions on Robotics and Automation, Vol.17, No.4, pp.377-390, 2001.

[8] G. Wasson, P. Sheth, M. Alwan, K. Granata, A. Ledoux, C. Huang, "User Intent in a Shared Control Framework for Pedestrian Mobility Aids", Proc. of the 2003 IEEE/RSJ International Conference on Intelligent Robots and Systems, Vol.3, pp.2962-2967, 2003.

[9] A. J. Rentschler, R. A. Cooper, B. Blaschm M. L. Boninger, "Intelligent walkers for the elderly : Performance and safety testing of VA-PAMAID robotic walker", Journal of Rehabilitation Research and Development, Vol.40, No.5, pp.423-432, 2003.

[10] Y. Hirata, A. Hara, K. Kosuge, "Motion Control of Passive Intelligent Walker Using Servo Brakes", Proc. of the IEEE Transactions on Robotics and Automation, Vol.23, No.5, pp.981-990, 2007.

[11] Y. Hirata, Z. Wang, K. Fukaya, K. Kosuge, "Transporting an Object by a Passive Mobile Robot with Servo Brakes in Cooperation with a Human", Advanced Robotics, Vol.23, No.4, pp.387-404, 2009.

[12] K. Fukaya, Y. Hirata, Z. D. Wang,K. Kosuge, Design and Control of A Passive Mobile Robot System for Object Transportation.", Proc. of the 2006 IEEE International Conference on Mechatronics and Automation, pp.31-36, 2006.

[13] Y.Hirata, H. Song, Z. Wang, K. Kosgue, "Control of Passive Object Handling Robot with Free Joint for Reducing Human Assistive Force", Proc. of the IEEE International Conference on Intelligent Robots and Systems, pp.1154-1159, 2007.

[14] M. Saida, Y. Hirata, K. Kosuge, "Motion Control of Passive Mobile Robot Consisting of Casters with Servo Brakes", Proc. of IEEE/RSJ International Conference on Intelligent Robotics and Systems, 2009.